

Southern Ocean sea ice and its wider linkages: insights revealed from models and observations

CLAIRE L. PARKINSON

*Oceans and Ice Branch/Code 971, NASA Goddard Space Flight Center, Greenbelt, MD 20771, USA
Claire.L.Parkinson@nasa.gov*

Abstract: Early conceptual models and global climate model (GCM) simulations both indicated the likelihood of an enhanced sensitivity to climate change in the polar regions, derived from the positive feedbacks brought about by snow and ice. As GCMs developed, however, the expected enhanced sensitivity has been more robust in the North Polar Region than the South Polar Region. Some recent increased-CO₂ simulations, for instance, show little change in Southern Ocean sea ice extent and thickness and much less warming in the Southern Ocean region than in the sea ice regions of the Northern Hemisphere. Observations show a highly variable Southern Ocean ice cover that decreased significantly in the 1970s but, overall, has increased since the late 1970s. The increases are non-uniform, and in fact decreases occurred in the last three years of the 1979–2002 satellite record highlighted here. Regionally, the positive trends since the late 1970s are strongest in the Ross Sea, while the trends are negative in the Bellingshausen and Amundsen seas, a pattern that appears in greater spatial detail in maps of trends in the length of the sea ice season. These patterns correspond well with patterns of temperature trends, but there is a substantial way to go before they are understood (and can be modelled) in the full context of global change.

Received 17 September 2003, accepted 5 July 2004

Key words: climate, climate change, polar amplification, remote sensing, sea ice, Southern Ocean

Introduction

Sea ice covers vast regions of the Southern Ocean, spreading over 18×10^6 km² in winter, although reducing to only 3×10^6 km² at its summer minimum (Fig. 1). The wintertime coverage far exceeds the 10.5×10^6 km² area of Europe and substantially exceeds the 14.2×10^6 km² area of the Antarctic continent that the Southern Ocean surrounds. The vast sea ice coverage has numerous impacts on the regional climate and on the plants and animals living in its vicinity, and hence examining the ice cover and its changes has become an important element of Earth System Science research.

Among the key questions in Southern Ocean sea ice studies are:

- What is the detailed seasonal cycle of the ice cover?
- What is the interannual variability in the ice cover?
- What are the decadal and longer time scale changes in the ice cover?
- How is the ice cover likely to change in the future?
- How closely is the ice cover tied to various oscillatory and non-oscillatory patterns in other components of the

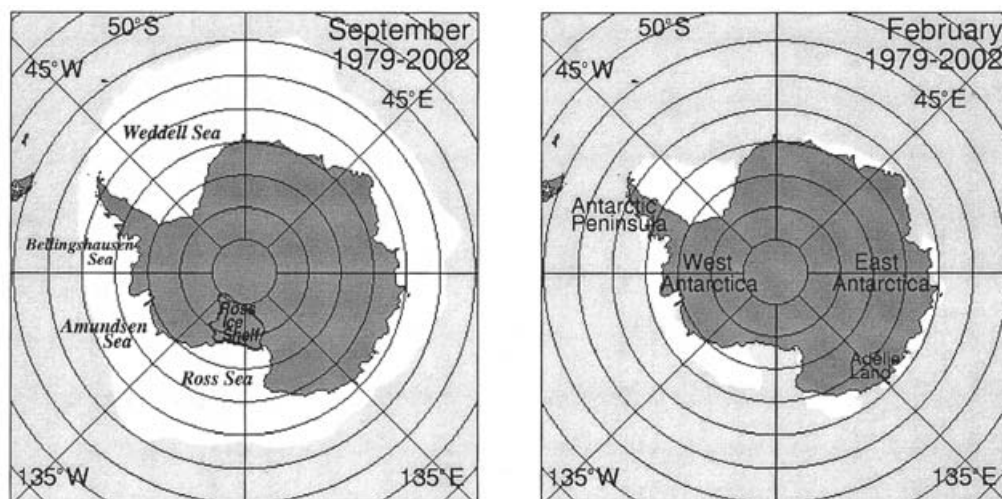


Fig. 1. Areal distribution (in white) of Southern Ocean sea ice in September and February, averaged over the 24-yr period 1979–2002 from satellite passive microwave data. September is frequently the month of maximum sea ice coverage, and February is almost always the month of minimum sea ice coverage. The maps also show the locations of places named in the text.

climate system?

What are the physiological adaptations allowing organisms to live within the ice?

How does the life within the ice affect the broader Southern Ocean ecosystem and climate?

Obtaining solidly based answers to any of the above questions, except the one on physiological adaptations, prior to the last few decades would have been impractical in view of the huge area involved and the limited tools available. However, with the development of satellite and computer technology in the latter half of the twentieth century, at least preliminary answers have become possible. Satellites provide platforms for routinely monitoring the entire ice cover and thereby provide data for answering the questions regarding the current state of the ice cover and its changes over the course of the satellite record. The observations alone, however, cannot provide answers regarding the future. For such answers, some theory or model is essential, even if the model is a simple hypothesis of persistence of current conditions or persistence of current trends. Similarly, the observations alone cannot answer questions regarding linkages among system components. For answers regarding linkages or the future, the tools proving the most useful are computer models, as these allow strict control of individual variables in a range of sensitivity studies and calculations running indefinitely into the future. Neither the satellite-derived data products nor the computer models are perfect, but they are providing important advances toward improved understandings, and this paper attempts to highlight some of these.

The next section reviews the impacts of sea ice on climate and life, and the following section reviews modelling results regarding polar amplification, the propagation of sea ice impacts beyond the Polar Regions, and the response of Southern Ocean sea ice to other climate variables. These reviews are followed by results from observations on the Southern Ocean sea ice cover, derived largely from satellite passive microwave data, a section comparing the Arctic and Antarctic sea ice covers, and a concluding summary and discussion.

Sea ice impacts on climate and life

Sea ice impacts the climate and life of the Southern Ocean in numerous ways. Among the most important climate impacts, the ice reflects most of the solar radiation incident on it, thereby contributing to keeping the region cool. It also is an effective insulator, restricting exchanges of heat, mass, and momentum between the ocean and the atmosphere. This restriction helps preserve ocean heat even in the midst of the polar winter and reduces wave motion and evaporation. Furthermore, the ice releases salt to the underlying ocean as it forms and ages, thereby increasing the salinity and density

of the water directly under the ice. When, depending on the initial vertical density profile, the densification causes the water immediately under the ice to become denser than the water below, the result can be overturning and sometimes even bottom water formation. More about bottom water formation in the Southern Ocean and its widespread importance can be found in Rintoul (1998) and in Jacobs (2004). Because the ice is less salty than the liquid ocean and because the net north–south motion of the ice is northward, the ice cover as a whole transports cold, relatively fresh water equatorward, creating an additional impact on the physical climate system. Furthermore, sea ice microbes produce substantial amounts of dimethylsulphoniopropionate (DMSP), which decomposes into dimethyl sulphide (DMS) (Trevena *et al.* 2000, Lizotte 2003). The DMS is oxidized to sulphuric acid in the atmosphere, providing sulphate aerosols and cloud condensation nuclei (Lizotte 2003).

Sea ice also affects a wealth of plant and animal life, including housing many microorganisms, serving as a platform for such animals as penguins and seals, restricting light to life forms beneath the ice, and insulating life beneath the ice from the cold polar atmosphere. Through a suite of physiological adaptations, assemblages of bacteria, algae, protists, viruses, and invertebrates thrive inside the ice itself, some in fact living their entire life cycles within the ice (e.g. Thomas & Dieckmann 2002, Lizotte 2003). Sea ice also releases algae to the water as it melts in spring and summer, and this release can lead to major algal blooms near the ice edge (e.g. Arrigo *et al.* 2002), although, at the same time, the presence of sea ice restricts sunlight to the underlying ocean and restricts the total level of Southern Ocean primary production (Arrigo & Thomas 2004). The sea ice organisms and their impact on algal blooms and primary productivity in turn impact animals all the way up through the food chain, from sub-ice metazoan fauna such as krill grazing on the ice algae (Loeb *et al.* 1997, Schnack-Schiel 2003) to much larger animals, including seals, whales, penguins, and a variety of flying birds (Croxall 1992, Smith *et al.* 1995, Arrigo *et al.* 2002, Ainley *et al.* 2003, Hofmann & Murphy 2004). The platform provided by the ice surface is also critical to many of the larger animals; e.g. Antarctic seals are born and nursed on the ice (either fast ice or sea ice), and penguins, snow petrels, and Antarctic petrels moult on the ice and exploit the ice platform for feeding purposes (Ainley *et al.* 2003). More on the organisms living within the ice, their life cycles, and their adaptations to the ice environment can be found in Lizotte (2003) and Schnack-Schiel (2003); and more on the importance of the ice to birds and mammals significantly affected by it can be found in Ainley *et al.* (2003) and Croxall *et al.* (2002).

Scientifically, sea ice has the further impact that because it can readily be monitored through relatively routine satellite observations, changes in the sea ice cover have the

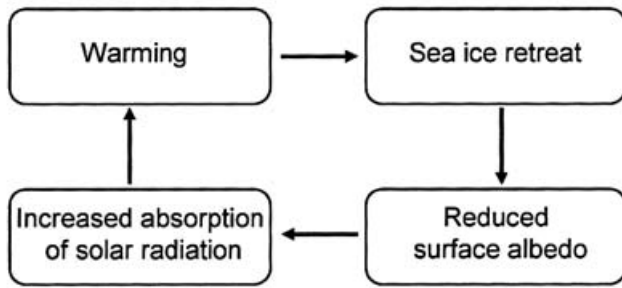


Fig. 2. Schematic of the ice albedo feedback, whereby the high albedo of sea ice (producing a reduced surface albedo upon sea ice retreat) results in a loop in which warming leads to further warming. Similarly, cooling leads to ice expansion, increased surface albedo, decreased absorption of solar radiation, and hence further cooling.

possibility of becoming early indicators of broader climate change (Parkinson 1991). This could be true whether or not climate changes are amplified in the Polar Regions, although it would be even more likely in the event of **such polar amplification**.

Insights from models

Evolving expectations regarding polar amplification of climate change

Both simple conceptual models and several global climate model (GCM) simulations have indicated the likelihood of an enhanced sensitivity to climate change in the Polar Regions. This enhancement comes about because of the abundance of ice and snow surfaces in the Polar Regions and the **positive feedbacks** brought about as the ice and snow covers expand and contract. For example, the contrast between the high reflectivities of snow and ice (albedos generally exceeding 50%) and the markedly lower reflectivities of the underlying land and liquid water surfaces (albedos often below 20%) means that, in general, the area-wide reflectivity of incident solar radiation increases as the ice and snow covers expand and decreases as they contract. In the case of sea ice, this contrast facilitates an initial warming or cooling being amplified through the positive feedback provided as the ice responds (e.g. Fig. 2) (Kellogg 1975, Goody 1980). Models incorporating ice and albedo changes thereby have a mechanism that tends toward amplified temperature changes in the Polar Regions.

The expected polar amplification has been simulated in a variety of studies. For instance, using a seasonal energy-balance climate model, Robock (1983) finds a clear polar amplification in the global warming produced by an increase in the solar constant and in the global cooling produced by a decrease in the solar constant. Furthermore, he finds this amplification to disappear when snow and ice feedbacks are disallowed. Similarly, using GCMs with

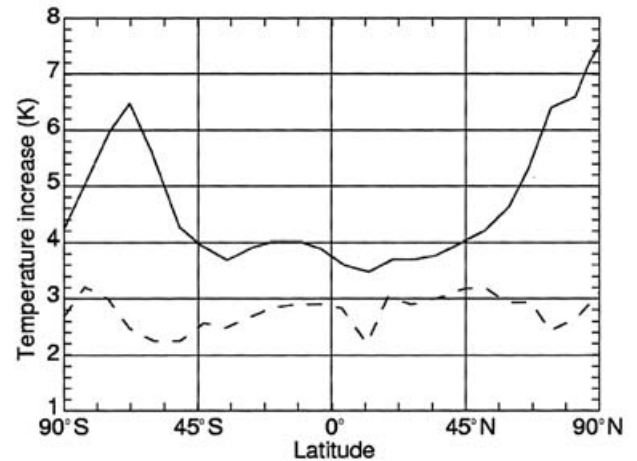


Fig. 3. Zonally averaged annual surface air temperature change simulated with the GISS GCM for a doubling of atmospheric CO_2 , both with (top curve) and without (bottom curve) coupled sea ice calculations included. The model used is the GISS atmospheric GCM coupled with a mixed layer ocean with specified ocean heat transport. [Updated from Rind *et al.* (1995).]

elaborate atmosphere models and simple mixed layer oceans, Manabe & Stouffer (1980, fig. 16) find a clear polar amplification in the warming simulated for a quadrupling of atmospheric CO_2 and Senior & Mitchell (1993, figs 11–12) find a clear polar amplification (especially in the winter hemisphere) in the warming simulated for a doubling of CO_2 under each of four cloud parameterizations. The Manabe & Stouffer study uses a model of the US National Oceanic and Atmospheric Administration (NOAA) Geophysical Fluid Dynamics Laboratory (GFDL), while the Senior & Mitchell study uses a model of the UK Hadley Centre for Climate Prediction and Research. The Goddard Institute for Space Studies (GISS) GCM, when run without a detailed ocean model, also simulates a strong polar amplification, as seen by the latitudinal distribution of global warming simulated for doubled atmospheric CO_2 (Fig. 3, top curve; Rind *et al.* 1995). Similarly to the Robock (1983) case, this polar amplification is largely eliminated when the sea ice calculations, and hence the feedbacks that accompany them, are eliminated (Fig. 3, bottom curve; Rind *et al.* 1995).

However, despite the tendencies of ice and snow feedbacks to lead to polar amplifications, as models have become more sophisticated, other feedbacks and processes have been incorporated that have in some cases reduced or eliminated polar amplifications of the simulated changes even when ice and snow feedbacks are incorporated. In particular, several coupled models show minimal warming in the Southern Ocean region in doubled CO_2 or other increasing CO_2 scenarios (Washington & Meehl 1989, Manabe *et al.* 1991, Cattle *et al.* 1992, Murphy & Mitchell 1995, Manabe & Stouffer 1999), in large part because in

this region oceanic convection mixes the surface warming down to substantial depths, on the order of 3000 m (Gordon & O'Farrell 1997). Washington & Meehl (1989, fig. 19) find a sharp contrast between the large warming (up to 8 K) in the north polar region and the lack of pronounced warming (generally under 1.5 K) in the Southern Ocean region for a CO₂ doubling in the US National Center for Atmospheric Research (NCAR) Community Climate Model (CCM). Murphy & Mitchell (1995, fig. 4b) find substantial warming in the North Polar Region but almost none in the Southern Ocean vicinity in response to a transient increase of CO₂ in the 2.75° latitude x 3.75° longitude UK Hadley Centre coupled 17-layer ocean, 11-layer atmosphere model, and Cattle *et al.* (1992) also find minimal warming in the Southern Ocean region under transient CO₂ increases with the Hadley Centre model once the 17-layer deep-ocean model is incorporated. Similarly, Stouffer *et al.* (1989) and Manabe *et al.* (1991, fig. 12a) report an inter-hemispheric asymmetry in the simulated response to a 1% yr⁻¹ increase in CO₂ compounded through a 100 yr simulation of a coupled model from the NOAA GFDL. The highest surface air temperature increases occur in the North Polar Region, establishing a north polar amplification, but, in marked contrast, the lowest surface air temperature increases anywhere around the globe occur in the region of the Southern Ocean. Manabe *et al.* (1991) and Gordon & O'Farrell (1997) explicitly address the relatively weak warming and weak sea ice decreases in the Southern Ocean. Specifically, they explain them on the basis of the Southern Ocean water being mixed to unusually deep levels, through convection and subgrid-scale vertical mixing. Thus the ocean warming spreads through a deeper layer than in other regions, leading to less surface warming in models that are properly simulating the vertical mixing than, for example, in models that impose a uniform mixed-layer depth. Another factor is a simulated reduction in poleward advection of warm waters in the Southern Hemisphere (Gordon & O'Farrell 1997).

Other factors are involved as well, as shown in Pollard & Thompson (1994) using a coupled GCM without deep ocean mixing. They use the NCAR Global Environmental and Ecological Simulation of Interactive Systems (GENESIS) model, which combines a 12-layer atmosphere model, a 6-layer soil model, a 3-layer snow model, a 6-layer sea ice model, and an ocean represented by a thermodynamic slab of thickness 50 m everywhere except in Hudson Bay, where the slab thickness is 25 m. When the model is run for control and doubled CO₂ cases without incorporating sea ice dynamics, they find strong polar amplification in surface air temperatures in both Polar Regions, especially in winter. However, when a cavitating-fluid sea ice dynamics model from Flato & Hibler (1990) is included in the calculations, the north polar amplification is similar to the amplification without ice dynamics, while the south polar amplification is significantly less (Pollard &

Thompson 1994). Hence in their case, reduced south polar amplification comes about through incorporation of sea ice dynamics, not through deep ocean mixing.

As a final example, Weatherly & Zhang (2001) use a Parallel Climate Model (PCM) combining an atmosphere GCM from NCAR, an ocean GCM from the Los Alamos National Laboratory, and a dynamic-thermodynamic sea ice model from the US Naval Postgraduate School. They run a 300-year control simulation with atmospheric CO₂ continually at 355 ppm and a 300-year increasing-CO₂ simulation in which CO₂ starts at 355 ppm, increases by 1% yr⁻¹ for the first 70 years, and is held constant at its doubled value of 710 ppm from year 70 onward. In both Polar Regions, the CO₂-induced surface air warming is greater in the winter than the summer, and in both seasons, the warming is, overall, significantly greater over the north polar sea ice than over the Southern Ocean sea ice. Over the Southern Ocean, the warming tends to be 0–1.5 K in the summer months and 0–3.5 K in the winter months, with the Weddell Sea experiencing greater winter warming, rising to 5 K in a small area of the eastern portion of the sea (Weatherly & Zhang 2001).

Thus, although expectations of a polar amplification of climate change had been simulated in both hemispheres with several models in the 1980s and early 1990s, as models grew more sophisticated in their treatment of the oceans and incorporated sea ice dynamics, the simulated strong polar amplification tended to remain in the Northern Hemisphere but not in the Southern Hemisphere. This tendency toward reduced south polar amplification, however, reversed somewhat when Flato & Boer (2001) introduced an improved parameterization for ocean mixing by Gent & McWilliams (1990) into the Canadian Centre for Climate Modelling and Analysis (CCCma) coupled GCM, transitioning from the CGCM1 to the CGCM2. The CGCM1 had simulated weak overall warming in the Southern Ocean (with patches of cooling) for the 2041–60 period versus 1971–90. The improved CGCM2, in contrast, simulated substantial Southern Ocean warming and polar amplification in both Polar Regions (Flato & Boer 2001). Such sensitivity of south polar amplification to various model adjustments leaves considerable uncertainty as to whether incorporation of further processes and further improvements in the parameterizations in different GCMs will re-establish a consensus south polar amplification or not. At the moment, most state-of-the-art GCMs are simulating a far stronger polar amplification in the North Polar Region than in the South Polar Region.

Simulated global impacts of sea ice

The Rind *et al.* (1995) study mentioned earlier because of its determination that eliminating sea ice calculations greatly reduces polar amplification in GISS GCM doubled-CO₂ results is centred on the broader role of sea ice in global

warming simulations. Specifically, Rind *et al.* (1995) examine the role of sea ice (in both hemispheres) in simulated climate sensitivity to doubled atmospheric CO₂ by running the GISS GCM under control and doubled CO₂ conditions both with and without coupled sea ice calculations included. Without sea ice calculations, and hence without the corresponding positive feedbacks, the doubled CO₂ simulation attains a 2.61 K global warming versus the control run. With sea ice calculations, the same model simulates greater doubled-CO₂ warming at all latitudes and a 4.17 K global warming (Fig. 3). Since the sea ice treatment was the only change between the two pairs of model runs, the inclusion of sea ice in the model calculations accounts for 1.56 K of the 4.17 K global warming, or 37%. This illustrates that in the simulations of the GISS GCM, changes in the polar sea ice covers can propagate to have significant impacts globally. Since sea ice extends over less than 5% of the globe, this demonstrates the high sensitivity that the results of a GCM can have to individual parameterizations within the model, even when those parameterizations directly apply to a relatively small area of the globe.

The GISS GCM was further used for a more complete examination of the sensitivity of the simulated surface air temperatures to sea ice concentrations, with the model run with realistic current sea ice concentrations, then run again 16 times with ice concentrations artificially adjusted by

increases and decreases of 1, 2, 4, 7, 20, 30, 40, and 50% (Parkinson *et al.* 2001). Globally, the impact of the ice concentration changes is, on average, to warm the surface air by 0.107 K for each 10% ice concentration decrease, with much greater changes occurring in individual regions and seasons (Parkinson *et al.* 2001).

Modelled trends in sea ice

Although the climate community has been far more interested in modelling temperature changes in response to such possibilities as doubled CO₂, there have also been some studies focusing on potential sea ice changes. In particular, Parkinson & Bindschadler (1984) use a stand-alone sea ice model to simulate the response of the Southern Ocean ice to uniform atmospheric temperature decreases and increases. For temperature changes ranging from a decrease of 1 K to an increase of 5 K, they find a hemispherically averaged winter ice-edge retreat of 1.4° latitude for each 1 K increase in temperature. Ice areas and volumes at maximum ice extent are cut approximately in half with a 5 K temperature increase, and minimum summer ice is reduced to zero in all except the Amundsen and Weddell seas with a 3 K temperature increase (Parkinson & Bindschadler 1984).

More recently, responses of the Southern Ocean sea ice to increasing CO₂ have been simulated with fully coupled

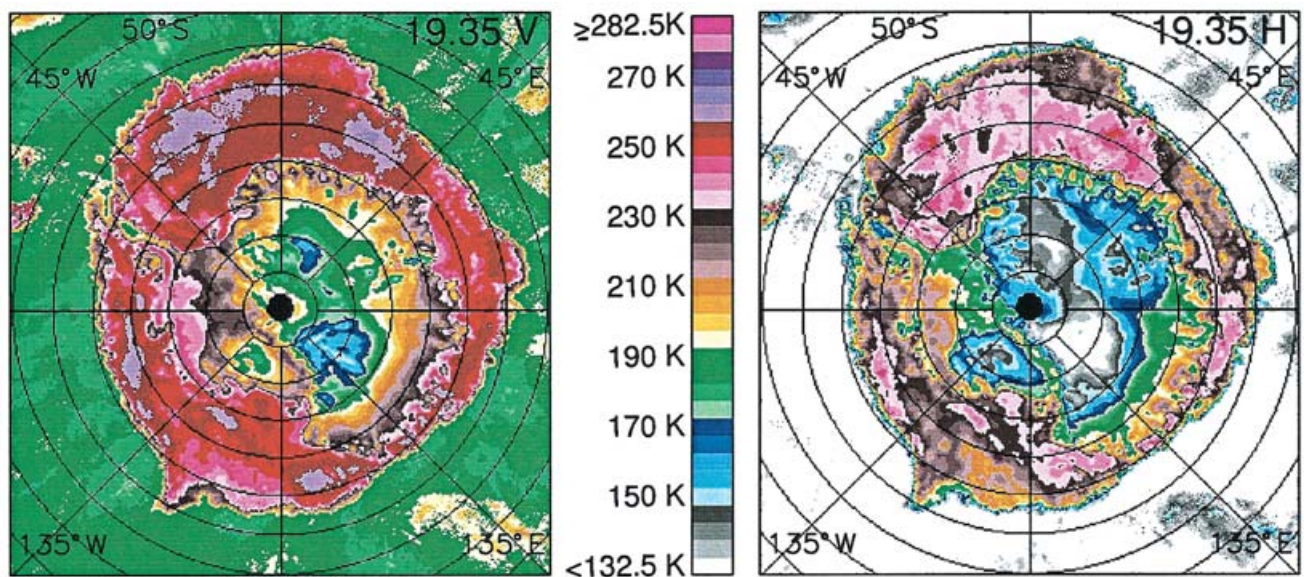


Fig. 4. Satellite SSM/I 19.35 GHz brightness temperature images for September 1, 2002, illustrating the ready identification of the sea ice edge from satellite microwave data. The sharp contrasts between the 19.35 GHz emissivities of ice and water, at both vertical (left image) and horizontal (right image) polarizations, translate to sharp contrasts between the brightness temperatures of ice-infested waters and ice-free waters. For the vertical-polarization data, the brightness temperatures are generally above 232 K for ice-infested waters and below 195 K for ice-free waters. For the horizontal-polarization data, the ice edge shows up even more strongly with the selected colour scale, because ice-free waters generally have brightness temperatures below the 132.5 K cut off at the bottom of the scale, while ice-infested waters generally have brightness temperatures exceeding 150 K, making the ice-infested waters stand out against the generally white background of the ice-free waters (greys and blues within the ice-free region identify areas with storms or other atmospheric interference).

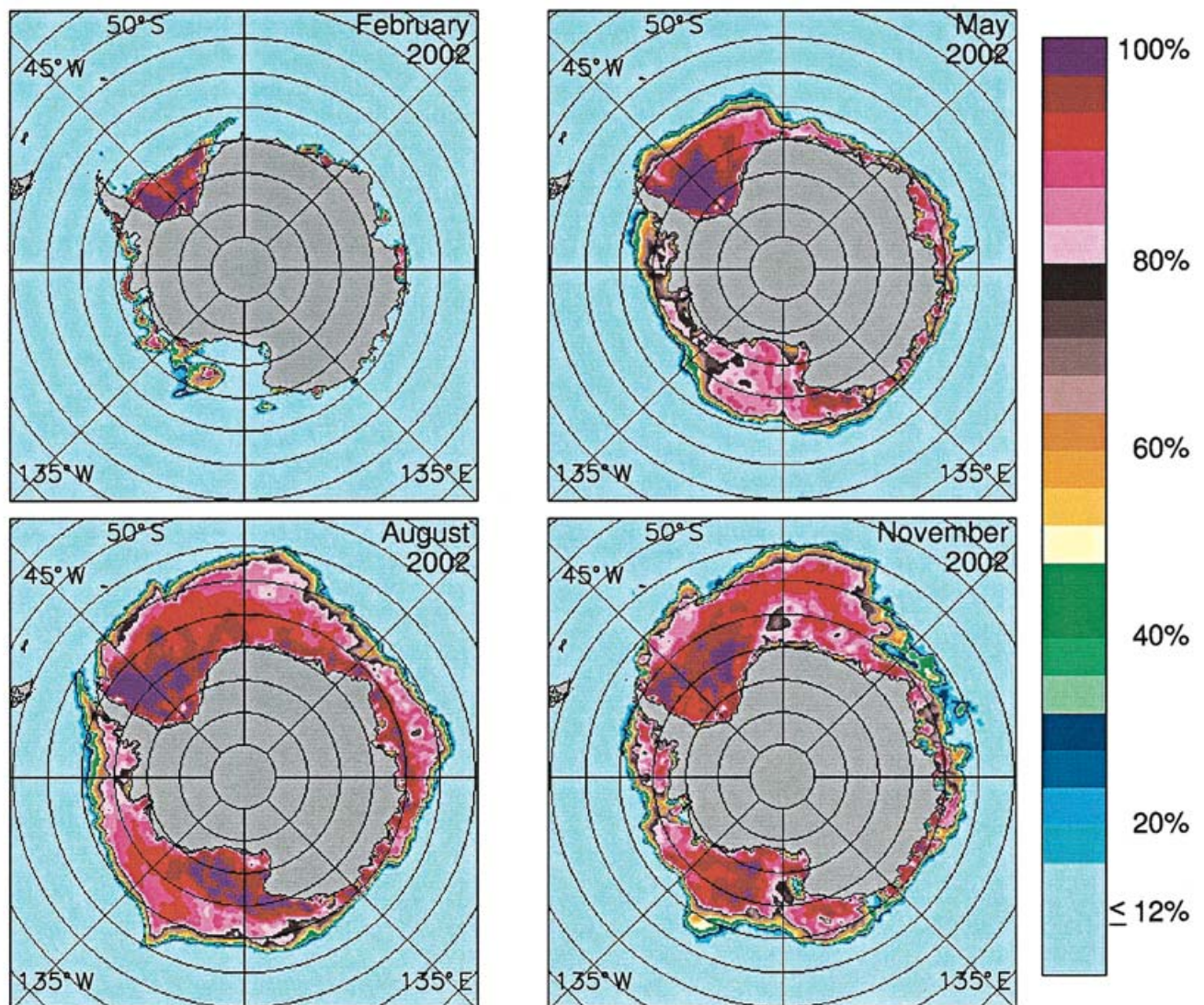


Fig. 5. Monthly average sea ice concentrations for February, May, August and November 2002, derived from SSMI satellite passive microwave data.

GCMs. Results from the comprehensive Australian Commonwealth Scientific and Industrial Research Organization (CSIRO) coupled model show sea ice decreasing in both hemispheres, although the Southern Ocean ice decreases far less than the Northern Hemisphere ice (Gordon & O'Farrell 1997). Specifically, in a 105-yr simulation with transient CO_2 increases of 1% per year starting at year 30, Southern Ocean sea ice volume does not decrease appreciably during the first 35 years, and at the end of the run has decreased only by about 10%, while the Northern Hemisphere ice decreases by over 60%. The hemispheric contrast is in line with the greater simulated surface atmospheric warming in the Northern Hemisphere, with warming particularly pronounced in the Arctic (Gordon & O'Farrell 1997).

Weatherly & Zhang (2001), using the already mentioned Parallel Climate Model (PCM), simulate, in their control case, sea ice coverage that tends to be too extensive in both polar regions, although not excessively thick. Doubled CO_2 is simulated to have a significant impact on Arctic sea ice thickness (thinning it on average by about 0.5 m) but much less impact on Southern Ocean ice thickness (0.05 m average thinning) or either Arctic or Southern Ocean ice areas (about 10% decreases). The lack of significant impact of increased CO_2 on Southern Ocean sea ice is found in sample simulations using the Hadley Centre HadCM3, Geophysical Fluid Dynamics Laboratory GFDL_R30_c, Canadian Centre for Climate Modelling and Analysis CGCM2, and NCAR CSM 1.3 models as well (Cubasch *et al.* 2001).

Results from observations

Data sources

The remoteness of the Southern Ocean, the harshness of the polar conditions, and the large area involved make it particularly difficult to obtain records of the full Southern Ocean ice cover through *in situ*, ship, or aircraft observations. As a result, the sea ice records prior to the early 1970s are quite limited, both spatially and temporally. Satellite passive microwave technology, however, has so dramatically changed the data collection situation that the full Southern Ocean sea ice cover can now be routinely monitored every day, at a spatial resolution on the order of 25 km or better. The reasons for this include not just the development of satellite technology but also the microwave properties of ice, water, and the atmosphere. Most crucially, at many microwave wavelengths, sea ice has a substantially different emissivity than does liquid water, thereby providing a sharp contrast in the satellite passive microwave data and allowing the ice distribution to be readily identified (Fig. 4). Additionally, because the microwave radiation is being emitted from within the Earth-atmosphere system, there is no necessity for solar illumination and thus data can be collected at any time of day or night, a particularly important feature for the Polar Regions in view of the extended length of the polar night. Furthermore, because the radiation at many microwave frequencies can pass through most clouds and the rest of the atmosphere easily, passive microwave data regarding sea ice can be collected under most weather conditions. This allows much more complete data records of sea ice and other surface variables than from instruments measuring in visible or infrared wavelengths, for which cloud cover obscures the surface information.

Satellite passive microwave data have been collected since the launch of the Electrically Scanning Microwave Radiometer (ESMR) on board NASA's Nimbus 5 satellite in December 1972. However, the record had substantial gaps in the 1970s, until the launch of the Scanning Multichannel Microwave Radiometer (SMMR) on the Nimbus 7 satellite

in late October 1978. The SMMR collected data every other day for most of the period from its launch until mid-August 1987, by which time the first of the Special Sensor Microwave Imagers (SSMIs) had been launched (in June 1987) on a satellite of the US Defense Meteorological Satellite Program (DMSP). Several SSMIs have been launched since then, collecting data on a daily basis. The combined SMMR/SSMI record provides Southern Ocean sea ice information from late October 1978 to the present. In 2002, two Advanced Microwave Scanning Radiometers (AMSRs) were launched, provided by Japan's National Space Development Agency (NASDA), subsequently consolidated into the Japan Aerospace Exploration Agency (JAXA). The first AMSR was launched on NASA's Aqua satellite on 4 May 2002, as part of the Earth Observing System (EOS), and is labelled the AMSR-E. The second AMSR was launched on 14 December 2002 on Japan's Advanced Earth Observing Satellite II (ADEOS II).

Many other satellite instruments, measuring visible, infrared, and microwave wavelengths, are also providing valuable information about the Southern Ocean sea ice. The passive microwave record is emphasized here because of providing the best long-term record of changes in the full Southern Ocean ice cover. However, visible and infrared measurements from instruments such as the Landsat Thematic Mapper Plus (TM+), the Système Pour l'Observation de la Terre (SPOT) Haute Resolution Visible (HRV), the Advanced Very High Resolution Radiometer (AVHRR), and the Moderate Resolution Imaging Spectroradiometer (MODIS) and active microwave measurements from Synthetic Aperture Radar (SAR) obtain sea ice information at higher spatial resolutions than the passive microwave measurements, thereby allowing more spatially detailed case studies. The reader is referred to Kramer (2002) for discussions of these and other instruments and capabilities.

Seasonal cycle and interannual variability

Figures 5–6 illustrate the seasonal cycle of Southern Ocean sea ice coverage, as derived from SMMR and SSMI data. The ice coverage generally reaches its minimum near the end of February, in late summer, and its maximum in August, September, or October, in late winter or early spring. Figure 5 presents monthly averaged maps of derived sea ice concentrations (percent areal coverages) for February, May, August and November 2002. The concentrations are estimated to have an accuracy of about $\pm 7\%$ and vary within approximately that range depending on which sea ice algorithm is used to convert from the satellite radiative data to sea ice concentrations. Figure 6 presents a plot of the yearly cycle of monthly average ice extent (integrated area of pixels with ice concentration at least 15%), averaged for the 24-yr period 1979–2002. For the 24-yr average, minimum monthly ice extent is 2.98 x

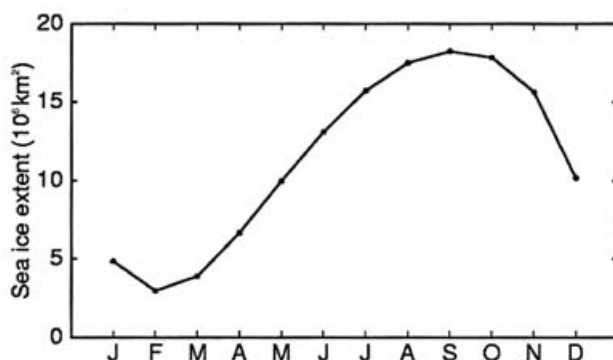


Fig. 6. Average annual cycle of monthly average sea ice extents for the Southern Ocean for the years 1979–2002, derived from SMMR/SSMI satellite passive microwave data.

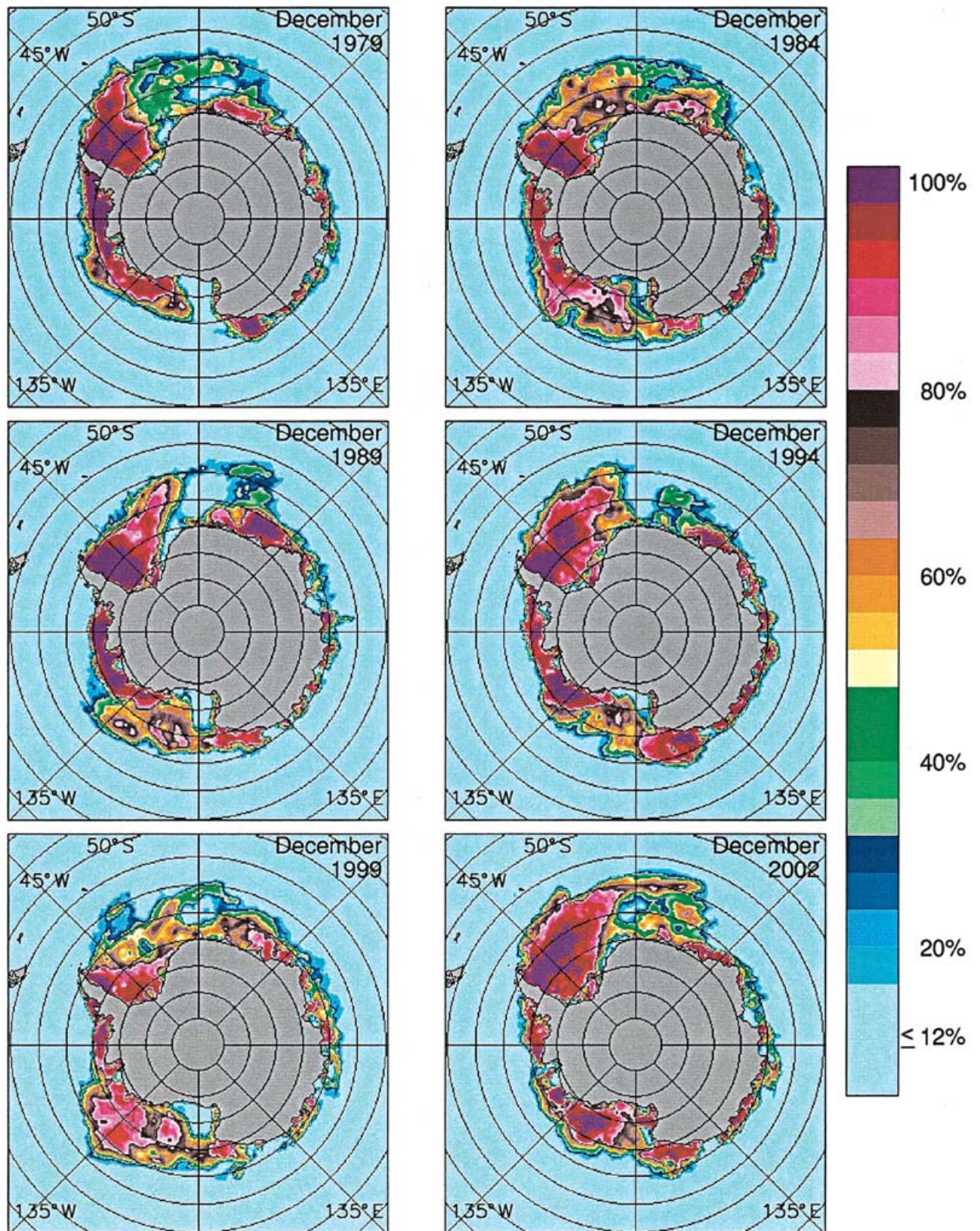


Fig. 7. Monthly average December sea ice concentrations for 1979, 1984, 1989, 1994, 1999 and 2002, derived from SMMR/SSM/I satellite passive microwave data.

10^6 km^2 , in February, and maximum monthly ice extent is $18.23 \times 10^6 \text{ km}^2$, in September, with ice growth more gradual than ice decay and ice decay particularly strong from November to December and December to January (Fig. 6).

One aspect of the Southern Ocean sea ice cover that has been brought into sharp relief by the satellite data is the significant amount of interannual variability. To illustrate this, Fig. 7 presents maps of December sea ice concentrations for 1979 and every five years after that through 1999, plus for 2002. These maps show a high level of variability in this late spring/early summer month, when the ice cover is rapidly decaying. Interannual variability is not as prominent in the peak winter months but is nonetheless quite noticeable in all months.

Ice extent trends

Interesting as the seasonal cycle and interannual variability (e.g. Figs 5–7) might be, of greater interest for most climate studies are the longer term trends in the ice cover. Indeed, when Kukla & Gavin (1981) published a 12-month running mean of Southern Ocean sea ice coverage for the period 1973–80, even though it covered only eight years it received considerable attention, because of revealing a sharp decline in ice extents and hence perhaps being indicative of global warming. In view of the gigantic seasonal cycle (Fig. 6), time series of monthly average ice extents highlight simply that cycle; the 12-month running mean removes the seasonal cycle and highlights the interannual fluctuations and the trend. Kukla & Gavin (1981) used a dataset from the US Navy-NOAA Joint Ice Center, based on visible, infrared, and ESMR microwave satellite data, along with

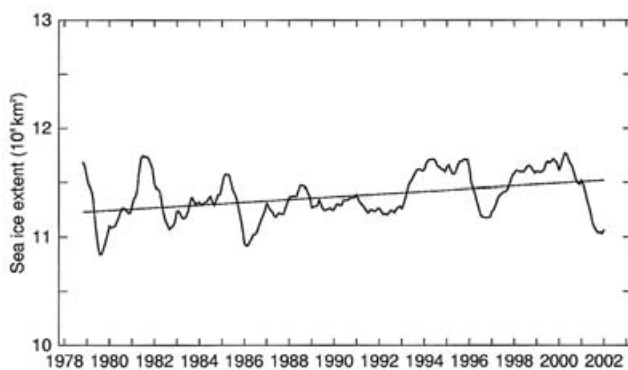


Fig. 8. 12-month running mean of the Southern Ocean sea ice extents from November 1978 through December 2002, derived from the SMMR/SSM/I satellite passive microwave data, and the corresponding line of linear least squares fit. The first point plotted is the 12-month average for November 1978–October 1979. Each tick mark on the x-axis corresponds to the mid-point of the year identified, so that the yearly average values are plotted at the respective tick marks. The slope of the least squares fit line is $12\,380 \pm 1730 \text{ km}^2 \text{ yr}^{-1}$.

Table I. Reported trends in Southern Ocean sea ice extents from the SMMR/SSM/I satellite passive microwave record. The values in the last two lines are updates through the end of 2002 of the Zwally *et al.* (2002) values and were obtained by the author and D.J. Cavalieri, in an ongoing updating of the sea ice time series.

Source	Period covered and averaging	Trend value
Björge <i>et al.</i> 1997	11/78–8/95, monthly	$-8000 \pm 7000 \text{ km}^2 \text{ yr}^{-1}$
Cavalieri <i>et al.</i> 1997	11/78–12/96, monthly	$14\,300 \pm 2600 \text{ km}^2 \text{ yr}^{-1}$
Watkins & Simmonds 2000	11/78–12/96, daily	$15\,100 \text{ km}^2 \text{ yr}^{-1}$
Zwally <i>et al.</i> 2002	11/78–12/98, monthly	$11\,180 \pm 4190 \text{ km}^2 \text{ yr}^{-1}$
Zwally <i>et al.</i> 2002	1/79–12/98, yearly	$10\,950 \pm 6950 \text{ km}^2 \text{ yr}^{-1}$
This paper	11/78–12/02, monthly	$8170 \pm 3240 \text{ km}^2 \text{ yr}^{-1}$
This paper	1/79–12/02, yearly	$8690 \pm 5590 \text{ km}^2 \text{ yr}^{-1}$

conventional, non-satellite observations, and found the 12-month running mean of the area with ice concentration exceeding 1 octa (12.5%) to have decreased from $13.5 \times 10^6 \text{ km}^2$ in 1973 to below $11 \times 10^6 \text{ km}^2$ in 1980 (Kukla & Gavin 1981). Not long after the Kukla & Gavin publication, however, extension of the dataset through the end of 1981 and reanalysis showed that the decreases had not continued and in fact that the ice cover had partially rebounded, with ice extent increases from 1979 to 1981 (Zwally *et al.* 1983, using ESMR, SMMR, and Navy-NOAA Joint Ice Center data). After examining the 1973–82 data, Ropelewski (1983) concluded that reliable identification of longer term trends than the record itself is precluded by the large year-to-year variability and the relatively short period of the data record. Although we now have a much longer record, in view of the considerable interannual variability (e.g. Fig. 7), the cautions of Ropelewski (1983) remain appropriate.

Figure 8 presents a 12-month running mean of the Southern Ocean sea ice extents for the period November 1978–December 2002, using the SMMR/SSM/I data record. Variability is prominent, but since the overall trend is positive, clearly the ice extent decreases found by Kukla & Gavin (1981) did not continue through the 1980s and 1990s (Fig. 8).

Because the SMMR/SSM/I time series is the most consistent long-term dataset available for the Southern Ocean sea ice cover, it is the one used for Fig. 8 and is also the one used by several groups over the past decade to derive Southern Ocean sea ice trends (Table I). Trends vary depending on the period covered and on the averaging interval (e.g. Table I). The values provided in the last two lines of Table I are updates through 2002 of the Zwally *et al.* (2002) trends through 1998, using the same algorithm and analysis methods. The decreases in ice coverage toward the end of the record (Fig. 8) result in a noticeable decrease in the overall trend for the extended record compared to the record through 1998, e.g. with the yearly average trend decreasing from $10\,950 \pm 6950 \text{ km}^2 \text{ yr}^{-1}$ to $8690 \pm 5590 \text{ km}^2 \text{ yr}^{-1}$ ($0.77 \pm 0.49\%$ per decade) and the trend calculated from the monthly averages decreasing even further (Table I). Stammerjohn & Smith (1997) also show SMMR/SSM/I

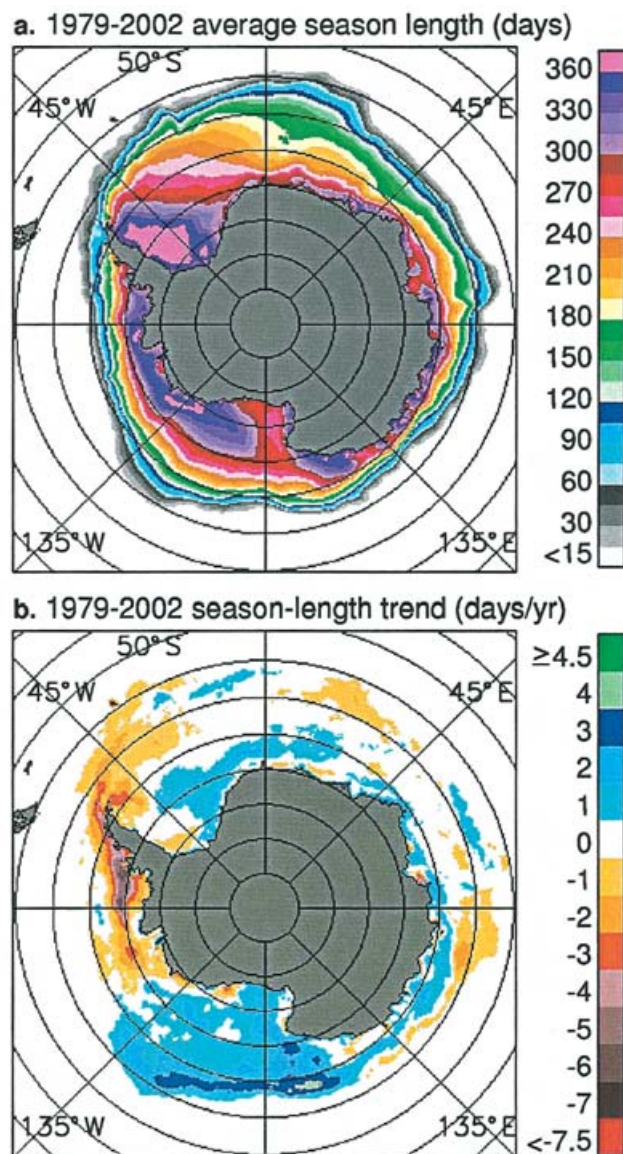


Fig. 9. Length of the Southern Ocean sea ice season and its trends: **a.** average ice season lengths over the period 1979–2002, and **b.** trends over the period 1979–2002. Season lengths are calculated for each year based on SMMR/SSMI satellite passive microwave data, and the trend at each pixel is calculated as the slope of the line of linear least squares fit through the 24 yearly season-length values.

plots with a positive trend (for 1979–94), but they do not include a trend value.

Because of the predominance of publications using the SMMR/SSMI record, the increase in Southern Ocean sea ice coverage since late 1978 (e.g. Fig. 8 and most entries of Table I) has become widely recognized. However, the Southern Ocean ice decreases in 1973–77 were large enough that the ice increases during the SMMR/SSMI period do not come close to compensating for them, leaving an overall negative trend for the full 1973–2000 period (Folland *et al.* 2001) or the full 1973–2002 period (Waple &

Lawrimore 2003, Cavalieri *et al.* 2003), assuming that the pre-1979 record is adequately homogenous with the higher-quality SMMR/SSMI record.

Examined spatially, the positive trends in the SMMR/SSMI record are strongest in the Ross Sea and weaker in the Weddell Sea and off the East Antarctic coast, while the trends are negative in the Bellingshausen and Amundsen seas to the west of the Antarctic Peninsula (e.g. Stammerjohn & Smith 1997, Zwally *et al.* 2002). Because some regions exhibit negative trends and others positive trends, the regional differences partially compensate each other, with a result that the magnitude of the ice-extent trend for the Southern Ocean as a whole is considerably less than the magnitude for some individual regions. For instance, over the 1979–98 period, the $10\,950 \pm 6950 \text{ km}^2 \text{ yr}^{-1}$ trend for the Southern Ocean yearly average ice extents (Table I) is 38% less than the $17\,600 \pm 7560 \text{ km}^2 \text{ yr}^{-1}$ corresponding trend for the Ross Sea from the same dataset (Zwally *et al.* 2002). The combined Bellingshausen and Amundsen seas also have a higher magnitude trend, at $-13\,290 \pm 5260 \text{ km}^2 \text{ yr}^{-1}$, than the Southern Ocean as a whole (Zwally *et al.* 2002). More spatial details can be seen, however, by shifting focus from ice extents to the length of the sea ice season.

Length of the sea ice season

The length of the sea ice season is defined as the number of days per year with sea ice coverage and is calculated from the SMMR and SSMI data on a pixel-by-pixel basis with a criteria of ice concentration needing to be at least 15% for classification as an ice day (Parkinson 2002). Figure 9a presents a map of the average length of the sea ice season over the 1979–2002 period. The largest region of perennial sea ice coverage is in the western Weddell Sea, and in general the ice season length decreases as one moves equatorward from the Antarctic coast (Fig. 9a).

Figure 9b presents a map of the trends in the length of the sea ice season, calculated at each pixel as the slope of the line of linear least squares fit through the 24 season-length values for the years 1979–2002. This map reveals shortening sea ice seasons throughout almost the entire Bellingshausen and Amundsen seas and in the north-western Weddell Sea, lengthening sea ice seasons throughout most of the Ross Sea and in the south-eastern Weddell Sea, and a mixed pattern of shortening and lengthening sea ice seasons around much of East Antarctica (Fig. 9b). This pattern corresponds well with the spatial pattern of temperature trends, as shown by Vaughan *et al.* (2003) with an earlier, similar version of Fig. 9b from Parkinson (2002), covering the period 1979–99. The Peninsula region is the one region in the Antarctic with a strong record of temperature increases (Thompson & Solomon 2002, Vaughan *et al.* 2003), matching well with the shortening sea ice seasons in the Bellingshausen,

Amundsen and western Weddell seas (Fig. 9b).

Arctic/Southern Ocean comparisons

The sea ice covers of the two Polar Regions are similar in many respects but also have notable contrasts. Both have huge seasonal cycles that dominate over long-term trends and that reach continent-sized areas each winter; both have ice thicknesses predominantly under 5 m; both are in constant flux, as winds and waves move the ice floes and open and close leads and polynyas; and both have significant interannual variability. However, the Arctic ice cover is centred in the central North Polar Region, with its expansion outward greatly confined by the surrounding North American and Eurasian continents, while the Southern Ocean ice is not confined in its equatorward expansion but cannot reach poleward of 78°S because of the presence of the Antarctic continent. These geographic differences contribute to the greater seasonal range in Antarctic ice extent (typically from 3×10^6 km² in February to 18×10^6 km² in September (Fig. 6)) than in Arctic ice extent (typically from 7×10^6 km² in September to 15×10^6 km² in March (Parkinson & Cavalieri 2002)), the larger amount of multiyear ice in the Arctic (where ice floes can survive for years within the Arctic Basin before drifting out through Fram Strait or other passageways), and the generally thicker ice in the Arctic (where ice floes 2.5–5 m thick are common) than in the Antarctic (where most sea ice is thinner than 2.5 m).

Both polar ice covers host an abundance of life forms that are an important part of the marine ecosystem, and both serve as important platforms from which other life forms operate. Still, there are significant ecosystem differences, the most frequently highlighted one being the presence of polar bears wandering atop the Arctic ice versus the presence of penguins in the Antarctic. This and other Arctic/Antarctic differences in mammal and bird populations are detailed in Ainley *et al.* (2003). Within the ice, rotifers and nematodes are abundant in Arctic sea ice but almost nonexistent in Antarctic sea ice, where the dominant metazoan fauna are copepods and acoel turbellarians. This and other contrasts in the organisms living within the sea ice of the two polar regions are detailed in Schnack-Schiel (2003).

The observation-based ice extent time series for the two Polar Regions show similar interannual and regional variabilities over the course of the satellite record but very different overall hemispheric behaviours. In particular, the SMMR/SSM/I record showing increases in Southern Ocean sea ice extents since late 1978 (e.g. Fig. 8) reveals higher magnitude, statistically significant decreases in the Arctic ice extent over the same time frame (e.g. Johannessen *et al.* 1995, Parkinson *et al.* 1999, Deser *et al.* 2000). Also, the sharp contrast in the Southern Ocean from major ice decreases in the 1970s to lesser magnitude increases since

1978 is not found in the Arctic, where there were, overall, decreases both before and after 1978. For the full 1973–2002 period, both hemispheres overall show ice extent decreases, with the Arctic trend, at $-30\,000$ km² yr⁻¹, having double the magnitude of the Southern Ocean trend (Cavalieri *et al.* 2003).

Summary and discussion

This paper reviews some of the impacts of Southern Ocean sea ice on other aspects of the climate system, examines some of the sea-ice-related issues addressed by climate modellers, and provides a summary of Southern Ocean sea ice coverage and changes as revealed through satellite passive microwave data. Major advances have been made both in numerical modelling and in satellite observations over the past several decades and, as a result, much new knowledge has been obtained about the Southern Ocean sea ice and other aspects of the climate system. However, as models have become more sophisticated, earlier results (such as the expectation of south polar as well as north polar amplification of climate change) have been called into question. Also, as observations have generated decades-long records of the full Southern Ocean ice cover, it has become apparent that interannual variability in the ice cover is quite significant (e.g. Fig. 7), complicating the identification of trends and linkages.

Still, the vastly improved database on sea ice and other elements of the global system, along with improved computer capabilities, are enabling a much improved picture of this system and the coupling within it. Among the named large-scale features of the global system with apparent sea ice connections are:

- The Southern Annular Mode (SAM), a large-scale, nearly zonally symmetric pattern of variability in the Southern Hemisphere extratropical atmospheric circulation. The SAM is characterized by fluctuations in the Southern Hemisphere circumpolar vortex. In model simulations, it generates sea ice variations on interannual to centennial time scales (Hall & Visbeck 2002, Thompson & Solomon 2002, Simmonds & King 2004).
- The Southern Oscillation, an irregular, interannual ‘seesaw’ in atmospheric sea level pressures over the tropical Pacific and Indian Oceans. Originally identified in 1924, the Southern Oscillation decades later was recognized as integrally tied with the oceanic El Niño phenomenon (Philander 1990, Glantz 1996). Simmonds & Jacka (1995) and Kwok & Comiso (2002) both explore possible connections between sea ice and the Southern Oscillation Index (SOI), finding that, temporally, correlations are strongest when the SOI leads the sea-ice-extent anomalies (Simmonds & Jacka 1995, using data from the 20 years 1973–92) and

that, regionally, correlations are strongest for the Bellingshausen, Amundsen and Ross seas (Kwok & Comiso 2002, using data from the 17 years 1982–98).

- The El Niño/Southern Oscillation (ENSO), the coupled ocean/atmosphere phenomenon linking the Southern Oscillation with the Pacific Ocean fluctuations between the unusually warm conditions in the central and eastern equatorial Pacific known as an El Niño and the cool conditions labelled La Niña. The El Niño was first named in the late 1800s, as a local phenomenon off the west coast of South America, and was recognized as a widespread oceanographic phenomenon and as coupled to the Southern Oscillation in the mid-1900s. Since then, the ENSO has been linked to weather conditions around the globe (Philander 1990, Glantz 1996), including Southern Ocean sea ice (Yuan & Martinson 2000, Watkins & Simmonds 2000, Rind *et al.* 2001, Yuan 2004). Rind *et al.* (2001) examine the sea ice/ENSO connection theoretically, as part of a modeling study simulating climate responses to changes in latitudinal sea surface temperature gradients. Their results suggest that less sea ice could be expected in the Pacific portions of the Southern Ocean during El Niño events. Using approximately 18 years of observations, Yuan & Martinson (2000) calculate that up to 34% of the variance in Southern Ocean sea ice extent is linearly related to ENSO. Watkins & Simmonds (2000) more specifically suggest that observed increases in Southern Ocean sea ice in the mid-1990s could be a response to the 1990–95 El Niño.
- The Antarctic Circumpolar Wave, a hypothesized system of coupled anomalies in atmospheric sea level pressure, meridional wind stress, sea surface temperature, and sea-ice concentrations that appear to propagate eastward with the circumpolar flow of the Antarctic circumpolar current, taking about 8–10 years to circle the South Pole (White & Peterson 1996, Gloersen & White 2001, Yuan 2004). First defined by White & Peterson (1996), the Circumpolar Wave's strength, persistence, and coherence remain topics of research. Animations of satellite data show signs of an eastward propagating wave in the sea ice cover for some limited periods and regions but generally not persisting through an encircling of the full Southern Ocean.
- The Antarctic Dipole, a quasi-stationary wave in the southern high latitudes with centres in the Atlantic and Pacific sectors of the Antarctic. Tied to the extended ENSO phenomenon, the Antarctic Dipole exhibits high temperatures and low sea ice in the Pacific centre and low temperatures and high sea ice in the Atlantic sector during a warm ENSO event (an El Niño) and the

opposite conditions during a cold ENSO event (a La Niña) (Yuan & Martinson 2000, 2001, Yuan 2004). First defined by Yuan & Martinson (2000, 2001), the Antarctic Dipole concept is related to the Antarctic Circumpolar Wave although suggests a quasi-stationary, standing wave pattern rather than a propagating wave as the dominant interannual variability in Southern Ocean sea ice and temperature.

With the Southern Ocean now felt likely to contain the major upwelling branch of the global thermohaline circulation (Pollard unpublished data), any major reduction in that circulation could significantly reduce heat to the undersurface of the ice and thereby reduce ice decay, increasing the ice cover. This in turn would block some of the ocean/atmosphere CO₂ flux, potentially reducing the significant draw down of atmospheric CO₂ into the Southern Ocean (e.g. Honjo 2004, Liss *et al.* 2004). Conversely, an enhancement of the thermohaline circulation could increase heat to the undersurface of the ice, decreasing the ice and increasing atmospheric CO₂ draw down. Any major changes in sea ice, through this mechanism or others, would affect the regional absorption of solar radiation and ocean-atmosphere exchanges, would affect the habitat of the organisms living within the ice (e.g. Thomas & Dieckmann 2002, Arrigo & Thomas 2004), with potential impacts propagating up through the food chain of the Southern Ocean (e.g. Croxall 1992, Hofmann & Murphy 2004), and could also affect Antarctic bottom water production and thereby impact, in the longer term, much larger regions of the world's oceans (e.g. Jacobs 2004). All these connections are far from fully understood or quantified, but paleoclimate evidence assures that far greater changes are possible in the Southern Ocean than any experienced during the period of instrumental records (Mackensen 2004), and the overwhelming likelihood is that these changes are integrally tied to those occurring in the rest of the global system.

Acknowledgements

The author thanks Nick DiGirolamo for assistance in the generation of the figures, the US National Snow and Ice Data Center (NSIDC) for archiving the ESMR, SMMR, and SSMI datasets, David Walton and two anonymous reviewers for comments on the manuscript, and Sharon Cooke for help in the production stage. This work was funded by the NASA Cryospheric Sciences Program, whose support is gratefully acknowledged.

References

- AINLEY, D.G., TYNAN, C.T. & STIRLING, I. 2003. Sea ice: a critical habitat for polar marine mammals and birds. In THOMAS, D.N. & DIECKMANN, G.S., eds. *Sea ice: an introduction to its physics, chemistry, biology and geology*. Oxford: Blackwell Science, 240–266.

- ARRIGO, K. & THOMAS, D. 2004. Large scale importance of sea ice biology in the Southern Ocean. *Antarctic Science*, **16**, 471–486.
- ARRIGO, K.R., VAN DIJKEN, G.L., AINLEY, D.G., FAHNESTOCK, M.A. & MARKUS, T. 2002. Ecological impact of a large Antarctic iceberg. *Geophysical Research Letters*, **29**, 10.1029/2001GL014160.
- BJØRGO, E., JOHANNESSEN, O.M. & MILES, M.W. 1997. Analysis of merged SMMR-SSM/I time series of Arctic and Antarctic sea ice parameters 1978–1995. *Geophysical Research Letters*, **24**, 413–416.
- CATTLE, H., MURPHY, J.M. & SENIOR, C.A. 1992. The response of Antarctic climate in general circulation model experiments with transiently increasing carbon dioxide concentrations. *Philosophical Transactions of the Royal Society of London*, **B338**, 209–218.
- CAVALIERI, D.J., GLOERSEN, P., PARKINSON, C.L., COMISO, J.C. & ZWALLY, H.J. 1997. Observed hemispheric asymmetry in global sea ice changes. *Science*, **278**, 1104–1106.
- CAVALIERI, D.J., PARKINSON, C.L. & VINNIKOV, K.Y. 2003. 30-Year satellite record reveals contrasting Arctic and Antarctic decadal sea ice variability. *Geophysical Research Letters*, **30**, doi:10.1029/2003GL018031.
- CROXALL, J.P. 1992. Southern Ocean environmental changes: effects on seabird, seal and whale populations. *Philosophical Transactions of the Royal Society of London*, **B338**, 319–328.
- CROXALL, J.P., TRATHAN, P.N. & MURPHY, E.J. 2002. Environmental change and Antarctic seabird populations. *Science*, **297**, 1510–1514.
- CUBASCH, U., MEEHL, G.A., BOER, G.J., STOUFFER, R.J., DIX, M., NODA, A., SENIOR, C.A., RAPER, S. & YAP, K.S. 2001. Projections of future climate change. In HOUGHTON, J.T., DING, Y., GRIGGS, D.J., NOGUER, M., VAN DER LINDEN, P.J., DAI, X., MASKELL, K. & JOHNSON, C.A., eds. *Climate change 2001: the scientific basis. Contribution of Working Group I to the Third Assessment Report of the Intergovernmental Panel on Climate Change*. Cambridge: Cambridge University Press, 524–582.
- DESER, C., WALSH, J.E. & TIMLIN, M.S. 2000. Arctic sea ice variability in the context of recent atmospheric circulation trends. *Journal of Climate*, **13**, 617–633.
- FLATO, G.M. & BOER, G.J. 2001. Warming asymmetry in climate change simulations. *Geophysical Research Letters*, **28**, 195–198.
- FLATO, G.M. & HIBLER III, W.D. 1990. On a simple sea-ice dynamics model for climate studies. *Annals of Glaciology*, **14**, 72–77.
- FOLLAND, C.K., KARL, T.R., CHRISTY, J.R., CLARKE, R.A., GRUZA, G.V., JOUZEL, J., MANN, M.E., OERLEMANS, J., SALINGER, M.J. & WANG, S.-W. 2001. Observed climate variability and change. In HOUGHTON, J.T., DING, Y., GRIGGS, D.J., NOGUER, M., VAN DER LINDEN, P.J., DAI, X., MASKELL, K. & JOHNSON, C.A., eds. *Climate change 2001: the scientific basis. Contribution of Working Group I to the Third Assessment Report of the Intergovernmental Panel on Climate Change*. Cambridge: Cambridge University Press, 99–181.
- GENT, P.R. & MCWILLIAMS, J.C. 1990. Isopycnal mixing in ocean circulation models. *Journal of Physical Oceanography*, **20**, 150–155.
- GLANTZ, M.H. 1996. *Currents of change: El Niño's impact on climate and society*. Cambridge: Cambridge University Press, 194 pp.
- GLOERSEN, P. & WHITE, W.B. 2001. Reestablishing the circumpolar wave in sea ice around Antarctica from one winter to the next. *Journal of Geophysical Research*, **106**, 4391–4395.
- GOODY, R. 1980. Polar process and world climate (a brief overview). *Monthly Weather Review*, **108**, 1935–1942.
- GORDON, H.B. & O'FARRELL, S.P. 1997. Transient climate change in the CSIRO coupled model with dynamic sea ice. *Monthly Weather Review*, **125**, 875–907.
- HALL, A. & VISBECK, M. 2002. Synchronous variability in the Southern Hemisphere atmosphere, sea ice, and ocean resulting from the Annular Mode. *Journal of Climate*, **15**, 3043–3057.
- HOFMANN, E.E. & MURPHY, E.J. 2004. Advection processes and effects on Antarctic marine ecosystems. *Antarctic Science*, **16**, 487–499.
- HONJO, S. 2004. Particle export and the biological pump in the Southern Ocean. *Antarctic Science*, **16**, 501–516.
- JACOBS, S.S. 2004. Bottom water production and its link with the thermohaline circulation. *Antarctic Science*, **16**, 427–437.
- JOHANNESSEN, O.M., MILES, M. & BJØRGO, E. 1995. The Arctic's shrinking sea ice. *Nature*, **376**, 126–127.
- KELLOGG, W.W. 1975. Climatic feedback mechanisms involving the polar regions. In WELLER, G. & BOWLING, S.A., eds. *Climate of the Arctic*. Fairbanks: Geophysical Institute, University of Alaska, 111–116.
- KRAMER, H.J. 2002. *Observation of the Earth and its environment: survey of missions and sensors*, 4th ed. Berlin: Springer, 1510 pp.
- KUKLA, G. & GAVIN, J. 1981. Summer ice and carbon dioxide. *Science*, **214**, 497–503.
- KWOK, R. & COMISO, J.C. 2002. Southern Ocean climate and sea ice anomalies associated with the Southern Oscillation. *Journal of Climate*, **15**, 487–501.
- LISS, P., CHUCK, A., TURNER, S. & WATSON, A. 2004. Air-sea gas exchange in Antarctic waters. *Antarctic Science*, **16**, 517–529.
- LIZOTTE, M.P. 2003. The microbiology of sea ice. In THOMAS, D.N. & DIECKMANN, G.S., eds. *Sea ice: an introduction to its physics, chemistry, biology and geology*. Oxford: Blackwell Science, 184–210.
- LOEB, V., SIEGEL, V., HOLM-HANSEN, O., HEWITT, R., FRASER, W., TRIVELPIECE, W. & TRIVELPIECE, S. 1997. Effects of sea-ice extent and krill or salp dominance on the Antarctic food web. *Nature*, **387**, 897–900.
- MACKENSEN, A. 2004. Changing Southern Ocean palaeocirculation and effects on global circulation. *Antarctic Science*, **16**, 369–386.
- MANABE, S. & STOUFFER, R.J. 1980. Sensitivity of a global climate model to an increase of CO₂ concentration in the atmosphere. *Journal of Geophysical Research*, **85**, 5529–5554.
- MANABE, S. & STOUFFER, R.J. 1999. The role of thermohaline circulation in climate. *Tellus*, **51A–B**, 91–109.
- MANABE, S., STOUFFER, R.J., SPELMAN, M.J. & BRYAN, K. 1991. Transient responses of a coupled ocean-atmosphere model to gradual changes of atmospheric CO₂. Part I: Annual mean response. *Journal of Climate*, **4**, 785–818.
- MURPHY, J.M. & MITCHELL, J.F.B. 1995. Transient response of the Hadley Centre coupled ocean-atmosphere model to increasing carbon dioxide. Part II: Spatial and temporal structure of response. *Journal of Climate*, **8**, 57–80.
- PARKINSON, C.L. 1991. Strengths and weaknesses of sea ice as a potential early indicator of climate change. In WELLER, G., WILSON, C.L. & SEVERIN, B.A.B., eds. *International conference on the role of the polar regions in global change: Proceedings, June 11–15, 1990, Fairbanks, Alaska*. Fairbanks: Geophysical Institute, University of Alaska, 1, 17–21.
- PARKINSON, C.L. 2002. Trends in the length of the Southern Ocean sea-ice season, 1979–99. *Annals of Glaciology*, **34**, 435–440.
- PARKINSON, C.L. & BINDSCHADLER, R.A. 1984. Response of Antarctic sea ice to uniform atmospheric temperature increases. In HANSEN, J.E. & TAKAHASHI, T., eds. *Climate processes and climate sensitivity*. Washington, DC: American Geophysical Union Monograph, **29**, 254–264.
- PARKINSON, C.L. & CAVALIERI, D.J. 2002. A 21 year record of Arctic sea-ice extents and their regional, seasonal and monthly variability and trends. *Annals of Glaciology*, **34**, 435–440.
- PARKINSON, C.L., CAVALIERI, D.J., GLOERSEN, P., ZWALLY, H.J. & COMISO, J.C. 1999. Arctic sea ice extents, areas, and trends, 1978–1996. *Journal of Geophysical Research*, **104**, 20 837–20 856.
- PARKINSON, C.L., RIND, D., HEALY, R.J. & MARTINSON, D.G. 2001. The impact of sea ice concentration accuracies on climate model simulations with the GISS GCM. *Journal of Climate*, **14**, 2606–2623.
- PHILANDER, S.G. 1990. *El Niño, La Niña, and the Southern Oscillation*. San Diego: Academic Press, 293 pp.
- POLLARD, D. & THOMPSON, S.L. 1994. Sea-ice dynamics and CO₂ sensitivity in a global climate model. *Atmosphere-Ocean*, **32**, 449–467.

- RIND, D., HEALY, R., PARKINSON, C. & MARTINSON, D. 1995. The role of sea ice in $2 \times \text{CO}_2$ climate model sensitivity. Part I: The total influence of sea ice thickness and extent. *Journal of Climate*, **8**, 449–463.
- RIND, D., CHANDLER, M., LERNER, J., MARTINSON, D.G. & YUAN, X. 2001. Climate response to basin-specific changes in latitudinal temperature gradients and implications for sea ice variability. *Journal of Geophysical Research*, **106**, 20 161–20 173.
- RINTOUL, S.R. 1998. On the origin and influence of Adélie Land bottom water. *Antarctic Research Series*, **75**, 151–171.
- ROBOCK, A. 1983. Ice and snow feedbacks and the latitudinal and seasonal distribution of climate sensitivity. *Journal of the Atmospheric Sciences*, **40**, 986–997.
- ROPELEWSKI, C.F. 1983. Spatial and temporal variations in Antarctic sea-ice (1973–82). *Journal of Climate and Applied Meteorology*, **22**, 470–473.
- SCHNACK-SCHIEL, S.B. 2003. The macrobiology of sea ice. In THOMAS, D.N. & DIECKMANN, G.S., eds. *Sea ice: an introduction to its physics, chemistry, biology and geology*. Oxford: Blackwell Science, 211–239.
- SENIOR, C.A. & MITCHELL, J.F.B. 1993. Carbon dioxide and climate: the impact of cloud parameterization. *Journal of Climate*, **6**, 393–418.
- SIMMONDS, I. & JACKA, T.H. 1995. Relationships between the interannual variability of Antarctic sea ice and the Southern Oscillation. *Journal of Climate*, **8**, 637–647.
- SIMMONDS, I. & KING, J.C. 2004. Global and hemispheric climate variations affecting the Southern Ocean. *Antarctic Science*, **16**, 401–413.
- SMITH, R.C., BAKER, K.S., FRASER, W.R., HOFMANN, E.E., KARL, D.M., KLINCK, J.M., QUETIN, L.B., PRÉZELIN, B.B., ROSS, R.M., TRIVELPIECE, W.Z. & VERNET, M. 1995. The Palmer LTER: A Long-Term Ecological Research program at Palmer Station, Antarctica. *Oceanography*, **8**, 77–86.
- STAMMERJOHN, S.E. & SMITH, R.C. 1997. Opposing Southern Ocean climate patterns as revealed by trends in regional sea ice coverage. *Climatic Change*, **37**, 617–639.
- STOUFFER, R.J., MANABE, S. & BRYAN, K. 1989. Interhemispheric asymmetry in climate response to a gradual increase of atmospheric CO_2 . *Nature*, **342**, 660–662.
- THOMAS, D.N. & DIECKMANN, G.S. 2002. Antarctic sea ice - a habitat for extremophiles. *Science*, **295**, 641–644.
- THOMPSON, D.W.J. & SOLOMON, S. 2002. Interpretation of recent Southern Hemisphere climate change. *Science*, **296**, 895–899.
- TREVENA, A.J., JONES, G.B., WRIGHT, S.W. & VAN DEN ENDEN, R.L. 2000. Profiles of DMSP, algal pigments, nutrients and salinity in pack ice from eastern Antarctica. *Journal of Sea Research*, **43**, 265–273.
- VAUGHAN, D.G., MARSHALL, G.J., CONNOLLEY, W.M., PARKINSON, C., MULVANEY, R., HODGSON, D.A., KING, J.C., PUDSEY, C.J. & TURNER, J. 2003. Recent rapid regional climate warming on the Antarctic Peninsula. *Climatic Change*, **60**, 243–274.
- WAPLE, A.M. & LAWRIE, J.H., eds. 2003. State of the climate in 2002. *Bulletin of the American Meteorological Society*, **84**(6), S1–S68.
- WASHINGTON, W.M. & MEEHL, G.A. 1989. Climate sensitivity due to increased CO_2 : experiments with a coupled atmosphere and ocean general circulation model. *Climate Dynamics*, **4**, 1–38.
- WATKINS, A.B. & SIMMONDS, I. 2000. Current trends in Antarctic sea ice: the 1990s impact on a short climatology. *Journal of Climate*, **13**, 4441–4451.
- WEATHERLY, J.W. & ZHANG, Y. 2001. The response of the polar regions to increased CO_2 in a global climate model with elastic-viscous-plastic sea ice. *Journal of Climate*, **14**, 268–283.
- WHITE, W.B. & PETERSON, R.G. 1996. An Antarctic circumpolar wave in surface pressure, wind, temperature and sea-ice extent. *Nature*, **380**, 699–702.
- YUAN, X. 2004. ENSO-related impacts on Antarctic sea ice: a synthesis of phenomenon and mechanisms. *Antarctic Science*, **16**, 415–425.
- YUAN, X. & MARTINSON, D.G. 2000. Antarctic sea ice extent variability and its global connectivity. *Journal of Climate*, **13**, 1697–1717.
- YUAN, X. & MARTINSON, D.G. 2001. The Antarctic Dipole and its predictability. *Geophysical Research Letters*, **28**, 3609–3612.
- ZWALLY, H.J., PARKINSON, C.L. & COMISO, J.C. 1983. Variability of Antarctic sea ice and changes in carbon dioxide. *Science*, **220**, 1005–1012.
- ZWALLY, H.J., COMISO, J.C., PARKINSON, C.L., CAVALIERI, D.J. & GLOERSEN, P. 2002. Variability of Antarctic sea ice 1979–1998. *Journal of Geophysical Research*, **107**, 10.1029/2000JC000733.